

MAX-PLANCK-INSTITUT FÜR RADIOASTRONOMIE

# Active Galactic Nuclei, Compact Radio Sources, VLBI

Brief reports<sup>1</sup> on recent research,  
period 1996–1997

Anton Zensus <sup>2</sup>	Scott Aaron <sup>3</sup>
Walter Alef	Geoffrey Bower
David Graham	Silke Britzen <sup>4</sup>
Thomas Krichbaum	Heino Falcke
Ivan Pauliny-Toth	Alexander Kraus
Richard Porcas	Andrew Lobanov
Eugen Preuss	Maria Massi <sup>5</sup>
Arno Witzel	Eduardo Ros

March 27, 1998

<sup>1</sup>edited by E. Preuss

<sup>2</sup>Director

<sup>3</sup>MPIfR/JIVE

<sup>4</sup>MPIfR/now: NFRA, Dwingeloo

<sup>5</sup>MPIfR/JIVE

# Contents

<b>1</b>	<b>Introduction</b>	<b>4</b>
<b>2</b>	<b>Compact radio sources in quasars, blazars and radio galaxies</b>	<b>6</b>
2.1	MM-VLBI of Active Galactic Nuclei — T.P. Krichbaum, W. Alef, D. Graham, A. Witzel, J.A. Zensus et al. . . . .	6
2.2	VLBI monitoring of the gamma-bright quasars 0420–014 and 0528+134 — S. Britzen, T.P. Krichbaum, A. Witzel, J. Roland, S. Wagner . . . . .	7
2.3	Intraday radio variability of blazars in total flux density and linear polarisation — A. Kraus, T.P. Krichbaum, A. Witzel, S. Wagner, A. Quirrenbach, B. Rickett, Bo Peng, S.J. Qian . . . . .	8
2.4	Spectral and flux density variations of the quasar 0836+710 and the blazar 0235+164 — A.P. Lobanov, A. Kraus, T.P. Krichbaum, C.E. Naundorf, M. Risse, P. Schneider, R. Wegner, A. Witzel, J.A. Zensus et al. . . . .	10
2.5	Spectral imaging: the distribution of synchrotron turnover frequencies in 3C273 and 3C345 — A.P. Lobanov, J.A. Zensus, E. Carrara . . . . .	12
2.6	Physical properties of ultracompact jets in 6 prominences	

2.13	Gigahertz-Peaked-Spectrum (GPS) radio sources — H. Falcke, A. Marecki, S. Garrington, A. Patnaik . . . . .	23
2.14	Jets in FR I radio galaxies — H. Falcke G. & M. Rieke, M. Ward, A.S. Wilson, C. Simpson, C. Henkel, J. Braatz, Y.P. Wang . . . . .	23
2.15	Radio quiet quasars — H. Falcke, A. Patnaik, W. Sherwood . . . . .	23
<b>3</b>	<b>Gravitational lenses</b>	<b>24</b>
3.1	Investigating the image morphology of the gravitational lens 2016+112 — R.W. Porcas, M. Garrett, S. Nair, and A. Patnaik . . . . .	24
3.2	Investigation of gravitational lens candidates 1030+074 — R.W. Porcas, A. Patnaik, E. Xanthopoulos, I. Browne, P. Wilkinson . . . . .	24
3.3	VLBI Polarimetry of gravitational lens systems — R.W. Porcas, A. Patnaik, and A. Kembal . . . . .	24
<b>4</b>	<b>High precision differential astrometry</b>	<b>26</b>
4.1	Relative astrometry of the quasar pair 1038+52A,B — R.W. Porcas and M.J. Rioja .	26
4.2	High precision differential astrometry with closure constraints — E. Ros, J.M. Marcaide, J.C. Guirado, M.I. Ratner, I. I. Shapiro, T.P. Krichbaum, A. Witzel, R.A. Preston . . . . .	27
<b>5</b>	<b>Nearby galaxies</b>	<b>30</b>
5.1	Compact radio cores in nearby galaxies — H. Falcke, L.C. Ho, A.S. Wilson, J. Ulvestad	30
5.2	Seyfert galaxies of type 2 — H. Falcke, A.S. Wilson, C. Simpson . . . . .	31
<b>6</b>	<b>The Galactic Center</b>	<b>32</b>
6.1	Spectrum of Sgr A* — H. Falcke, W.M. Goss, H. Matsuo, P. Teuben, J.-H. Zhao, R. Zylka . . . . .	32
6.2	Sagittarius A* — G. Bower, Backer, Wright, Doeleman, Rogers . . . . .	32
<b>7</b>	<b>Stars</b>	<b>33</b>
7.1	VLBI measurement of the size of dMe stars — W. Alef, A.O. Benz, M. Güdel . . . .	33
7.2	Activity cycles in UX Arietis — comparison with the Sun — M. Massi . . . . .	34
7.3	VLA observations of the field around the X-ray binary LSI+61303 — M. Massi . . . .	35
<b>8</b>	<b>VLBI techniques</b>	<b>36</b>
8.1	Total Power Corrections for Atmospheric Phase — G. Bower, Backer, Wright, Plambeck, Graham, Krichbaum and Conway . . . . .	36

8.2	Discovery of a systematic error in EVN VLBI — M. Massi et al. . . . .	37
8.3	Calibration of the instrumental polarization of VLB interferometers — M. Massi, M. Aaron, G. Tuccari, S. Orfei . . . . .	38

# 1 Introduction

The principal focus of the research to be reported about here is on the compact central emission components (radio cores) of luminous extragalactic radio sources associated with radio galaxies, blazars, and quasars. While the overall picture of these objects is understood in broad outline there are still many important questions waiting to be answered. There is reliable evidence that the physical ‘backbones’ in most of these radio sources are collimated outflows or ‘jets’ originating deep in the AGN (Active Galactic Nuclei) and often extending far beyond the boundaries of the parent galaxy where they can give rise to spectacular radio phenomena. It is in the very centre of the active galaxies that the key lies to understanding the radio phenomena and other manifestations of ‘nuclear activity’ across the electromagnetic spectrum.

Gaining insight into the working of the ‘radio nuclei’ and AGN in general has been one of the main drivers for the development of VLBI (Very-Long-Baseline Interferometry). With the as yet unequalled angular resolution of its global antenna arrays VLBI provides a very powerful tool for the investigations of small-scale phenomena and its potential is far from being exhausted. The ongoing development of VLBI implies: increasing the angular resolution to better than 0.1 milliarcsec through mm-VLBI and space VLBI as well as increasing the sensitivity so that sources with flux densities on the order of 10 mJy<sup>1</sup> or less can be imaged. This also means that it is now possible to determine the structure of the nonthermal emission from certain types of star.

The immediate results of VLBI measurements are, ideally, images in total intensity and linear polarisation. A measurable degree of polarisation is to be expected in many cases because the radio radiation is almost certainly emitted through the synchrotron mechanism by free electrons spiraling in magnetic fields. The information content of the observations can be increased considerably by measuring at several frequencies and repeatedly, in the quite frequent case of structurally variable sources. Further enhancement of the information content can be achieved by observations with local interferometers or ‘single dishes’. This outlines roughly the available instrumentation.

Questions to be answered include the following:

- what is the physical structure of the radio sources and their distinct components?
- where and how do jets form? how are they collimated on their way out of the AGN?
- what is the role of relativistic bulk motion inferred from apparent ‘superluminal motion’ of emission components and from rapid flux variability?
- what causes the ‘intraday variability’ of blazars, i.e. the fluctuations of total flux and linear polarisation on scales of less than 2 days?
- how are the radio properties related to features in other spectral domains? For example: many ‘superluminals’ are gamma-ray sources and intraday variability is observable across the electromagnetic spectrum!

A special asset of the VLBI techniques is its potential for highly precise differential astrometry, i.e. for measuring the spacing between reference points in neighbouring sources, (currently) as far apart as about a degree, with an accuracy of better than 0.1 milliarcsec. This allows one to check for proper motion or for a frequency dependence of the position of brightness maxima. It is also in principle possible to distinguish between stationary and moving components.

An important application of VLBI is the investigation of ‘gravitational lenses’. These are, in this context, foreground galaxies the gravitational field of which generates (in the most common case) multiple images of a distant background radio source, typically a quasar. VLBI polarimetry is especially a powerful tool, because the angle and the degree of any linear polarisation of an image element is unchanged by the lensing process, even if the resulting images are distorted and their structural axes

---

<sup>1</sup>1 Jy  $\equiv$  1 Jansky =  $10^{-26}$  W/m<sup>2</sup>/Hz

are rotated. This allows one to restrict the modelling of the mass distribution in the lens considerably.

The intrinsic luminosity of the strong radio sources we have assumed so far varies by about 4 orders of magnitude, the maximum being about  $10^{46}$  erg/s. If one considers all types of AGN, from the strongest through the weakest, then their emission power varies by at least 10 orders of magnitude. Owing to their growing sensitivity, VLBI observations of weak AGN at relatively close cosmic distances, are increasingly possible. The fundamental question to be answered here is: to what extent are the weaker AGN, as regards their basic physical processes, just scaled-down versions of the very luminous AGN? More specifically, are the main mechanisms of the ‘canonical model’, postulated to explain strong nuclear activity, also at work in weaker and very weak AGN? These are: collapse of matter onto a compact massive object (a black hole?) via a rotating accretion disk which at the same time may generate a collimated outflow of matter at high speed. To what extent is the orientation of the jets (through relativistic beaming and Doppler boosting or obscuration by dust tori) and their interaction with the galactic environment responsible for generating the various *o served* types of AGN. Some of the observed differences are probably just due to the way they are oriented towards us, so for example, strong radio galaxies and radio loud quasars or Seyfert galaxies of type I and II.

Of special interest is the very weak AGN in the centre of our Galaxy, at the position of the radio source Sagittarius A\* (Sgr A\*). The evidence, mainly based on near-infrared observations, that it harbours a black hole of about 1 Million solar masses, is becoming more and more conclusive. VLBI at short mm-wavelengths may possibly yield information about the black hole environment.

## 2 Compact radio sources in quasars, blazars and radio galaxies

### 2.1 MM-VLBI of Active Galactic Nuclei

*W. Alef, D. Graham, T.P.Krichaum, A. Witzel, J.A. Zensus, in colla oration with C.J. Schalinski (DLR, Berlin); A. Greve, M. Grewing, J. Wink (IRAM, Grenoble); K. Wiik, E. Valtaoja (Metsahovi); S. Doeleman, R. Phillips, A. Rogers (Haystack); S. Padin, K. Marvel (OVRO); D. Emerson (NRAO, Kitt Peak); R. Predmore (Qua in); D. Backer, M. Wright (Hat Creek); T. Beasley, V. Dhawan (NRAO, VLBA); L. Baath, R. Booth, J. Conway, F. Rantakyro (Onsala); A. Baudry (Bordeaux); A. Marscher, J. Moran (Boston); J. Alcolea, F. Colomer, P. de Vicente, J. Gomez-Gonzalez (Ye es); A. Al erdi, J.M. Marcaide, E. Ros (Spain); H. Hira ayashi, M. Inoue (Japan).*

VLBI observations at frequencies of up to **43 GHz** are made now routinely using the VLBA and several European telescopes, including the 100m radio telescope at Effelsberg. This yields images with 0.1-0.2 mas resolution and a dynamic range of more than 500:1. With such high dynamic range spectral index imaging (eg. for **4C 39.25**, **3C 345**) and studies of the spectral structure and spectral evolution in the inner parts of the jets are made possible.

VLBI observations at higher frequencies are more difficult and not yet standard. In the last years small arrays of typically 4-6 stations performed VLBI observations at **86 GHz**. By now up to 10 stations can observe simultaneously resulting in a 40 micro-arcsecond synthesized beam. Most of the new data are not yet fully analyzed, but the detection of about 20-30 sources already indicates that ultra compact structures with sizes less than 50 micro-arcseconds and jet bending are quite common features in AGN. This demonstrates that future 3mm-VLBI observations will allow detailed high resolution studies of the jet physics near the base of the jet.

The sensitivity limitations of the present 3 mm array allow detailed imaging only for sources brighter than 2-3 Jy. It can be expected, though, that future inclusion of phased arrays such as the interferometers at Plateau de Bure (IRAM) and at Owens Valley (OVRO) and Hat Creek (BIMA), will improve considerably the sensitivity of the 3mm array and the quality of the maps.

To date, the monitoring of the brightest objects (**3C273**, **3C279**, **3C454.3**, **0528+134**) is performed with a time sampling of about 1-3 observations per year. This shows rapid structural changes on sub-milliarsecond scales, which are often correlated with the observed broad band (gamma- to radio) flux density variations. In a large fraction of the objects imaged with mm-VLBI so far, the variations are very rapid and the data are undersampled in time. More frequent observations are needed in the future. In a few cases a correlation between the ejection of a new jet component and a rapid Gamma, X-ray and optical outburst has been seen (eg. **0528+134**, **3C273**, **0836+71**, **3C454.3**). This supports the idea of a broad band correlation of the flux density activity and jet physics for blazars in general. It also suggests that in gamma-bright quasars, the production of high energy electrons (MeV-TeV) and the relativistically beamed radiation from the inner jet are caused by related physical processes.

To push VLBI to even higher observing frequencies, pilot experiments were performed at **215 GHz** using a single antenna of the IRAM interferometer at Plateau de Bure and the 30 m telescope at Pico Veleta. In an experiment performed in March 1995, about 10 sources were detected for the first time at this frequency, among which is the compact radio source **Sgr A\*** at the Galactic Centre. The data on Sgr A\* yielded a first upper limit of its size at this short wavelength (0.1-0.2 mas). Unfortunately the remaining calibration uncertainties do not yet allow us to determine whether Sgr A\* is scatter broadened or not. For 1998 a new experiment is planned to confirm the detection and to improve the size estimate. With an event horizon of about 10 micro-arcsecond (for a  $2 \cdot 10^6 M_{\odot}$  black hole), 2 and 1 mm-VLBI observations of Sgr A\* bear the great potential of imaging directly the vicinity of a supermassive black hole.

## 2.2 VLBI monitoring of the gamma-bright quasars 0420–014 and 0528+134

*S. Britzen, T. Krichbaum, A. Witzel; in collaboration with J. Roland (IAP, Paris), S. Wagner (LSW, Heidelberg)*

A striking result of EGRET observations is the discovery that a relatively large number of strong superluminal radio sources are also bright and variable in the gamma regime. This immediately raises the question whether there are links between the phenomena in both domains. This question has been thoroughly investigated for **0420–014** and **0528+134**, both strong and strongly variable radio and gamma-ray emitters. The analysis was based on 3.6 cm VLBI data from geodetic campaigns for monitoring Earth rotation parameters (IRIS) which were compared with EGRET data. For 0420–014 (Fig. 1) VLBI maps were obtained for 9 epochs between 1989.3 and 1992.5, and for 0528+134 (Fig. 2) for 20 epochs between 1986.3 and 1994.1. In both sources superluminally moving jet components can be traced over time periods of several years on curved trajectories. Both sources exhibit component ejections preceding the time of observed gamma-ray flaring.

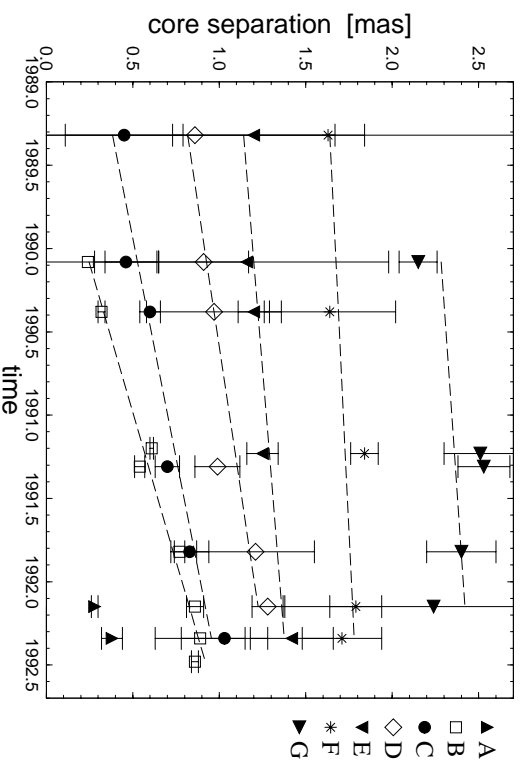


Figure 1: Core separation of emission components as a function of time for PKS 0420–014.

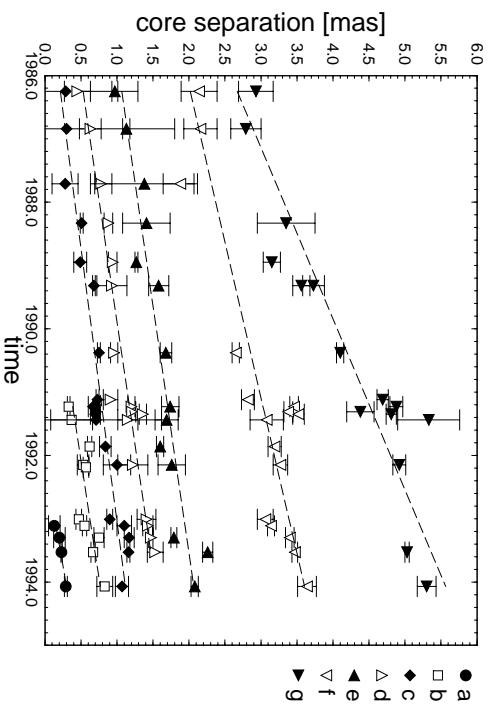


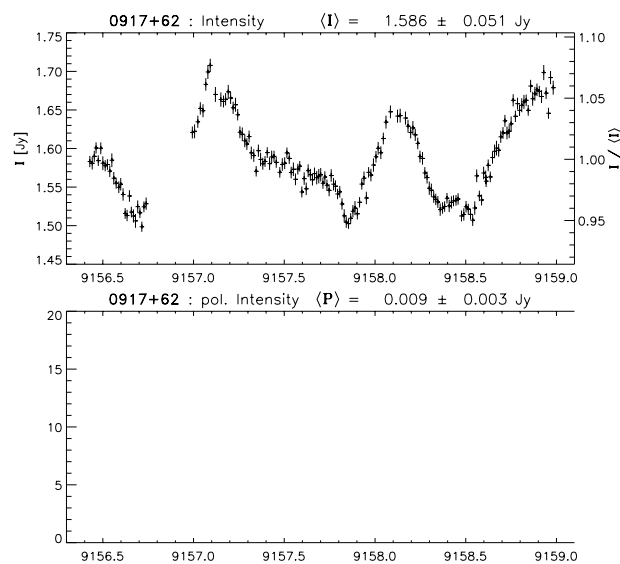
Figure 2: Core separation of emission components as a function of time for PKS 0528+134.

### 2.3 Intraday radio variability of blazars in total flux density and linear polarisation

*A. Kraus, T. Krichbaum, A. Witzel; in collaboration with S. Wagner (LSW, Heidelberg); A. Quirrenbach, B. Rickett (UCSD, San Diego); B. Peng, S.J. Qian (BAO, Peking)*

Even more than ten years after its discovery, the IDV phenomenon in blazars, meanwhile observed across the whole electromagnetic spectrum, is still puzzling. These variations — with typical timescales of less than two days and amplitudes  $\geq 1$  — can be found in a substantial fraction of all flat-spectrum radio sources with 6cm flux densities  $\geq 1$  Jy. It is still unclear whether they are caused by *source-intrinsic* or *source-extrinsic* mechanisms.

About 70 flat-spectrum sources have recently been observed with the 100 m radio telescope at 2.8, 6, and 11 cm wavelength; for about half of them the polarisation was also measured. A total of 250 light curves have been obtained with the following result: one third of the observed objects show IDV, often both in total flux density and linear polarization. Typical variations in the total flux density are on the order of 5–10%, but in some sources variations with amplitudes of up to 35% (e.g. in the quasar **0804+499**) have been observed. Variations of the polarized flux density are in most cases larger than those of the total flux density and can reach a factor of 2 (e.g. in **0917+624**). The polarization angle can vary from a few degrees up to  $100^\circ$  (e.g. in the quasar 0917+62). In one case a swing of  $180^\circ$  has been observed.



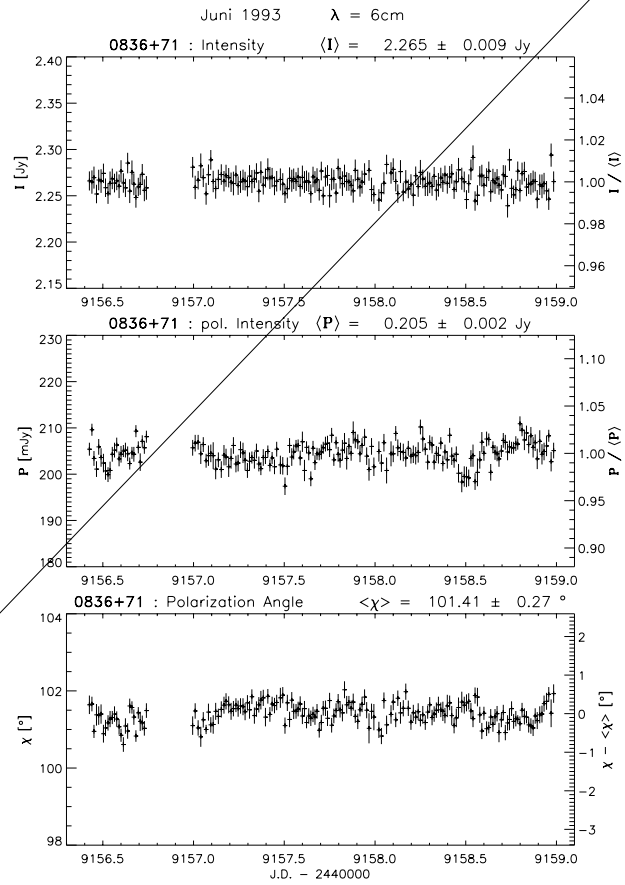
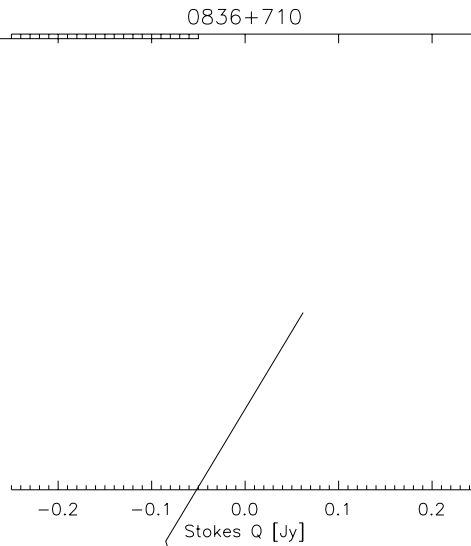


Figure 4: The quasar 0836+710 which showed no intraday variations in June 1993 at 6cm. Figure 5: Stokes-P



## 2.4 Spectral and flux density variations in the quasar 0836+710 and the blazar 0235+164

*A.P. Lo anov, A. Kraus, T.P. Krich aum, C.E. Naundorf, M. Risse, P. Schneider, R. Wegner, A. Witzel, J.A. Zensus (MPIfR); in colla oration with K. Otter ein, S.J. Wagner (LSW Heidelberg), A. Quirren ach (UCSD), H. Aller, and M. Aller (University of Michigan)*

High frequency VLBI-observations made following a strong Gamma/optical/radio outburst in the **quasar 0836+710** revealed the appearance of a new jet feature ejected shortly after the outburst and moving outwards at a constant apparent speed of  $\beta \sim 10$  (Fig. 6).

Monitoring of the variations in total radio spectrum showed a synchrotron self-absorbed spectral component consistent with adiabatic expansion in a relativistic plasma (see Fig. 7).

The spectral component has been further identified with the ejected jet feature, allowing to model the time lag between the outburst and the ejection by strong synchrotron self-absorption at the jet base. The model predicts that the jet radio-core is separated by  $\approx 15$  pc from the jet base. The jet plasma has bulk Lorentz factor  $\gamma_j \approx 12$ , and moves at about  $3^\circ$  angle to the line of sight. The corresponding jet opening angle derived from the expansion of the spectral component is  $\phi_j = 2.1^\circ$ . The ejection of a highly superluminal jet feature after the quasi-simultaneous optical/Gamma-flaring supports the idea that the Gamma-emission originates in the inner parts of a relativistic jet. The observed multi band energy output during and after the flare in 1992.1 allows to conclude that the Gamma and optical flaring activity are not sufficient to maintain the jet total power, but are connected with the observed jet radio emission. In this scheme, relativistic electrons are responsible for synchrotron emission in the optical and radio bands, and external Compton scattered photons produce the observed Gamma radiation.

An unusual radio variability has been discovered on timescales of several days in the **BL Lacertae type object AO 0235+164**. During a rapid ( $\sim 5$  days in duration) outburst a peculiar sequence of peaks in the emission at different frequencies has been observed: the maximum at 1.4 GHz precedes by  $\approx 0.7$  days the maximum at 8.4 GHz which, in turn, is followed by the maximum at 4.9 GHz, after  $\approx 0.1$  days (whereas the canonical scheme predicts that higher frequency emission should peak at earlier times). The peaks also become narrower and stronger at lower frequencies—a unique behavior not seen in other sources. Several models have been employed, in order to explain the observed variations. In one of them, the jet is assumed to consist of an ultrarelativistic ( $\gamma \approx 10$ ) electron-positron beam surrounded a thermal outflow with  $\beta \approx 0.4c$ . Perturbations developing in the beam may result in a precession-type motions, and subsequent variations of the Doppler factor can explain the observed sequence of peaks (Fig. 8). Additional spectral evolution of the emission (for instance, rapid cooling or strong in situ acceleration of emitting plasma) may be required, in order to explain the more narrow and stronger peaks observed at lower frequencies. Other possible mechanisms that may be responsible for the observed variations include free-free absorption by a foreground medium, interstellar scattering, and gravitational microlensing.

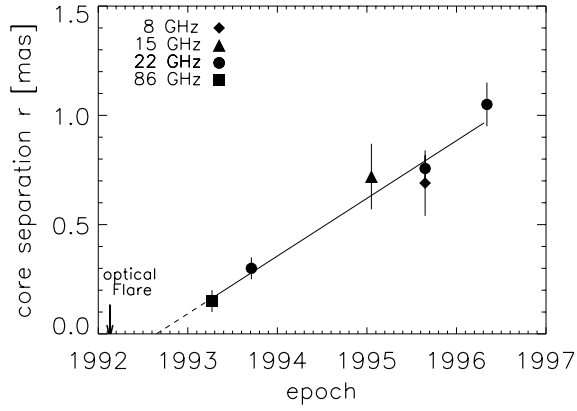


Figure 6: Relative core-separation of component B3 of the QSO 0836+710 plotted versus time. Symbols denote different frequencies: diamonds (8 GHz), triangles (15 GHz), circles (22 GHz), and squares (86 GHz). The solid line represents a linear fit with slope  $\mu = 0.26$  mas/yr, corresponding to superluminal motion with  $\beta_{\text{app}} = 10.8$ . Linear back-extrapolation (dashed line) yields component ejection near 1992.65. The arrow indicates the epoch of the peak of the optical flare (1992.13).

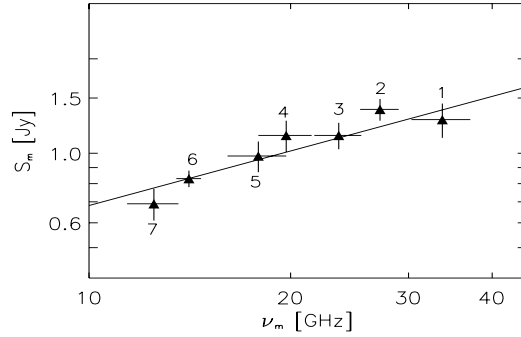


Figure 7: Spectral evolution of the flux density of the QSO 0836+710. Here the path of the spectral evolution of the turnover point in the  $S_m$ - $\nu_m$ -diagram is plotted. The labels 1-7 denote the individual spectral epochs. The straight line shows a power law fit ( $S_m \propto \nu_m^{0.58}$ ) to the data.

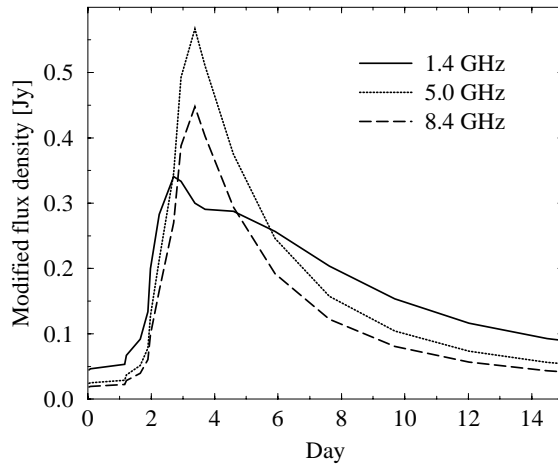


Figure 8: Short timescale variability in 0235+164. Here model lightcurves at 1.5, 4.9, and 8.4 GHz for a precession period  $P_0 = 200$  days and precession angle  $\Omega_0 = 5.7^\circ$  are shown. The time lags match the discrepancies between the maxima in the light curves observed.

## 2.5 Spectral imaging: the distribution of synchrotron turnover frequencies in 3C273 and 3C345 — A.P. Lobanov, J.A. Zensus, E. Carrara

*A.P. Lobanov, J.A. Zensus (MPIfR), and E. Carrara (University of São Paulo)*

Many contemporary jet models predict shocks and/or Kelvin–Helmholtz instabilities to form and propagate in relativistic jets. Both the shocks and instabilities are expected to produce characteristic patterns of velocity, pressure and particle density distributions in the jet. For detection of such patterns, mapping the distribution of the synchrotron turnover frequency,  $\nu_m$ , in relativistic jet has been implemented, based on multi–frequency VLBI data. A combination of the turnover frequency and turnover flux density,  $S_m$ , distributions also provides an estimate of magnetic field strength in the jet. The turnover frequency distributions have been mapped in 3C273 and 3C345. Figure 9 shows the turnover frequency and magnetic field profiles along the ridge line in 3C273. The peaks in the turnover frequency distribution coincide with the locations of the core (–13 mas) and the two most prominent features seen in the jet (–10.5 and –5 mas). The magnetic field profile calculated from the fitted distributions of  $S_m$  and  $\nu_m$  rises sharply at the locations of the jet components, which may be indicative of the presence of shocks. The fact that the peaks of the magnetic field are slightly offset and ahead of the peaks of the turnover frequency also supports the shock origin of the emission.

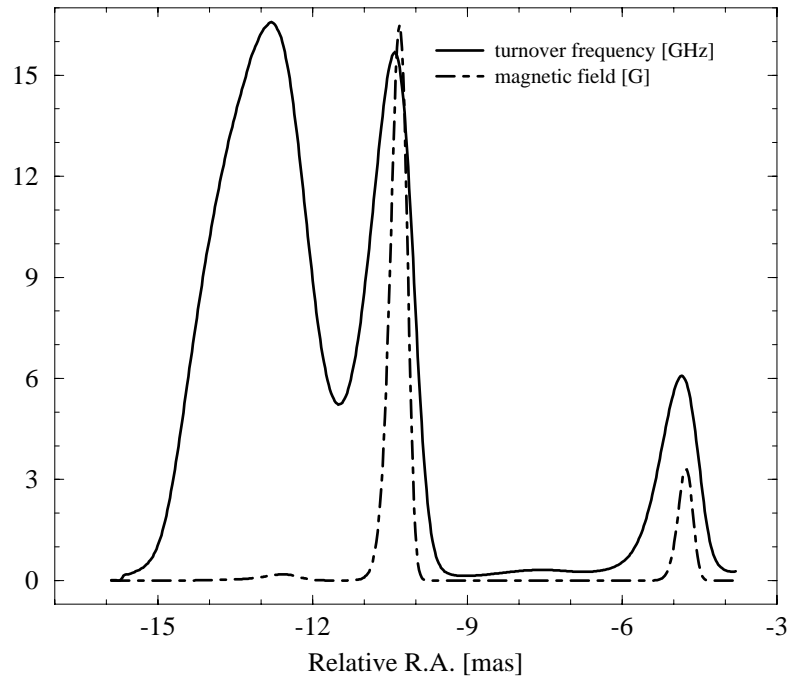


Figure 9: Turnover frequency and magnetic field profiles along the jet ridge line in 3C273. The core position is at –13 mas. The restoring beam width in the direction of the profile is about 1.7 mas.

## 2.6 Physical properties of ultracompact jets in 6 prominent radio sources — A.P. Lobanov, M.J. Rioja, L.I. Gurvits

*A.P. Lobanov (MPIfR), M.J. Rioja (IRA, Bologna), and L.I. Gurvits (JIVE, Dwingeloo)*

The properties of ultracompact jets in the prominent radio sources **Cygnus A**, **3C 309.1**, **3C 345**, **3C 395**, **4C 39.25**, and **1038+528 A** have been studied, using the frequency dependence of observed position of the optically thick jet core. Frequency dependent offsets of the core positions are used for calculating the luminosities, magnetic fields, and geometrical properties of the jets (cf. Fig. 10). Pressure and density gradients in the jets and in surrounding ambient medium are shown to be primary factors determining the observed properties of ultracompact jets. The opacity changes along the jet can be used for evaluating the physical conditions in the ultracompact jets, bringing an interesting connection to studies of the broad-line regions of AGN.

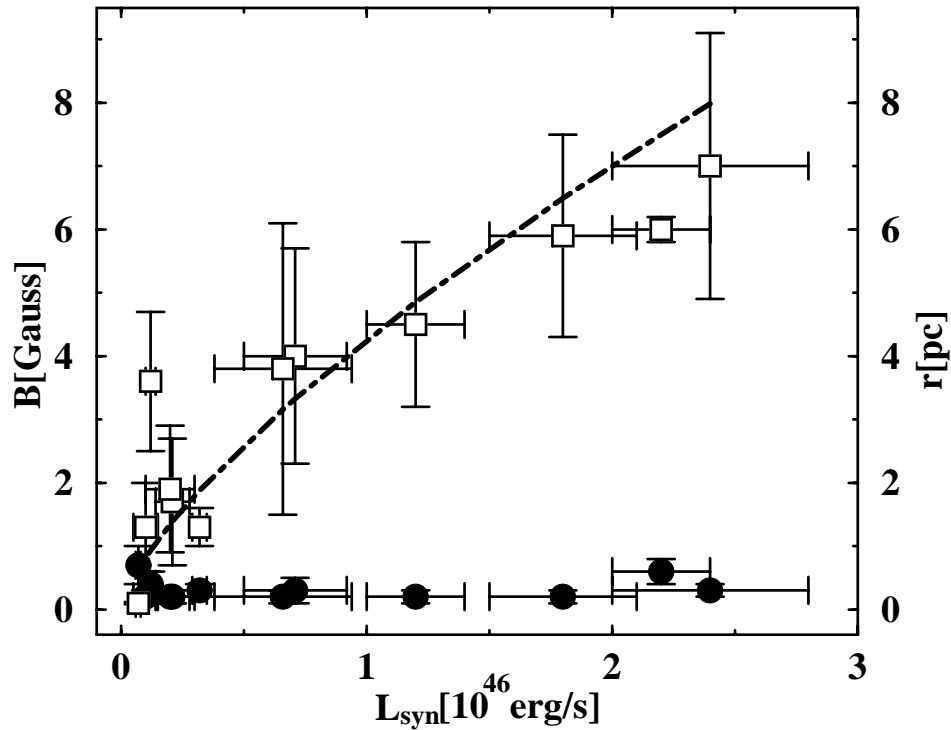


Figure 10: Dependence between the jet synchrotron luminosity and the properties of the jet core for six prominent radio sources (see text): magnetic field (filled circles) and distance of the core (squares) from the jet origin. The data are calculated for rest-frame frequency  $\nu' = 22$  GHz, for several prominent AGN. The dot-dashed line is  $r_{\text{core}} \propto L_{\text{syn}}^{2/3}$ .

VLBI

1981

3.1

enc

100

10

ed

1981

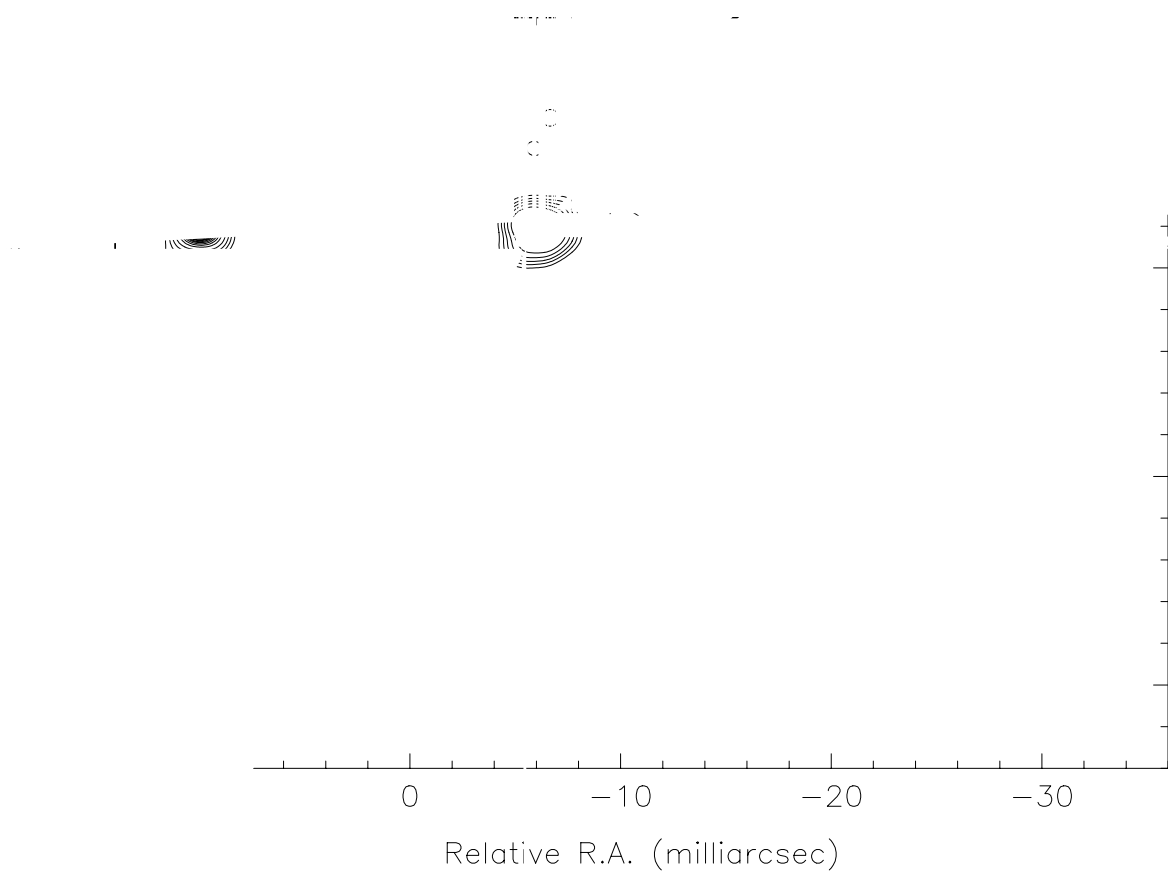
) was

= 100

source.

ation

Figure 11: Images of 3C 454.3 derived from global VLBI at 5 GHz (first epoch) and 8.4 GHz (last epoch). The



## 2.8 The Gamma-Ray Blazar NRAO 530

*G. Bower, Backer, Wright (UCB)*

Bower, Backer and Wright have studied the relationship between millimeter wave and high energy emission in the gamma-ray blazar NRAO 530. Gamma-ray blazars are radio-loud objects that have also been detected at energies greater than 100 MeV with the EGRET observatory.

Bower, Backer and Wright have monitored the millimeter and radio wavelength VLBI structure of NRAO 530 with the millimeter VLBI arrays, with the VLBA and with VSOP. NRAO 530 underwent a dramatic millimeter-wavelength flare in 1995 that has been studied extensively with VLBI (Bower et al. 1997). This flare was coincident with an increase in the gamma-ray activity. Currently the researchers are analyzing over 3 years of 3 mm and VLBA images that show the evolution of the jet following that flare. One or more new components were created during that flare. The most recent results show that the components may have decelerated to a subluminal speed following the initial outburst. If confirmed, this would be the first case of a subluminal gamma-ray blazar. Tracking the components should test the existence of this deceleration as well as give new information on the physical conditions in the jet.

## 2.9 VLBI of the FR II radio galaxy Cygnus A at 1.6, 22, and 43 GHz

*W. Alef, D. Graham, T.P.Krichaum, A. Witzel, J.A. Zensus; in collaboration with A. Rogers (Haystack), A. Greve (IRAM), and R. Booth (Onsala).*

VLBI monitoring at 1.6, 22, and 43 GHz yielded several new maps, tracing the jet and counter-jet from 0.07 to 300 parsec. The data show a frequency-dependent jet to counter jet ratio, which can best be interpreted by assuming a partially opaque fore-ground absorber, or torus that blocks the radiation from the counter jet but not from the jet. This lends new support to the idea that circumnuclear disks surround the cores of radio galaxies. The study of the apparent jet kinematics which yields velocities in the range of 0.1-0.7  $c$ , provides a tighter constraint on the jet inclination. On a simple relativistic jet hypothesis one finds that the jet is oriented within  $< 10^\circ$  of the plane of the sky. Most probably, the apparent acceleration seen in the jet is due to phase velocity effects or internal acceleration mechanisms; it cannot be due to geometrical effects.

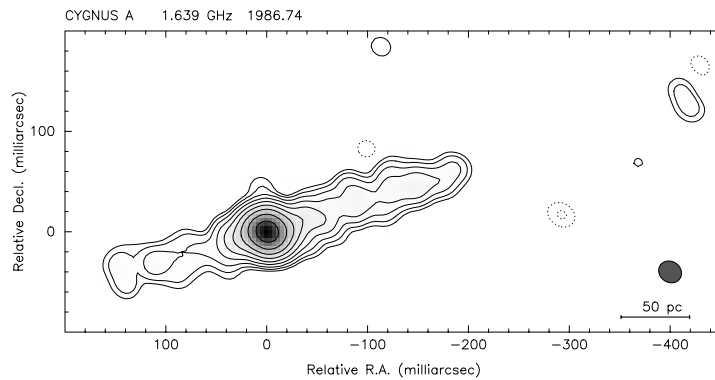


Figure 12: EVN-VLBI map of Cygnus A at 18 cm. Contour levels are -0.5, -0.25, 0.25, 0.5, 1, 2, 4, 8, 16, 32, 64 of the peak intensity of 0.27 Jy/beam.

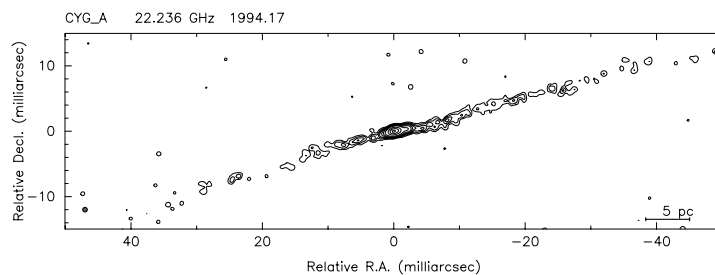


Figure 13: Jet- and counter-jet of Cygnus A in a tapered low angular resolution map. The figure shows the largest field of view ( $\sim 100 \times 30$  mas), which could be reliably imaged using the 22 GHz data of 1994.17. The map is displayed with a circular restoring beam of 0.7 mas size and a uv-tapering of 10 at  $800 M\lambda$  uv-distance. The contour levels are (-0.05), 0.05, 0.15, 0.3, 0.5, 1, 2, 5, 20, 50, and 90 of the peak intensity of 0.73 Jy/beam. The total flux density seen in the map is  $1.65 \pm 0.05$  Jy.

## 2.10 VLBI of the class II radio galaxy 3C111 at 3.6 cm and 7 mm

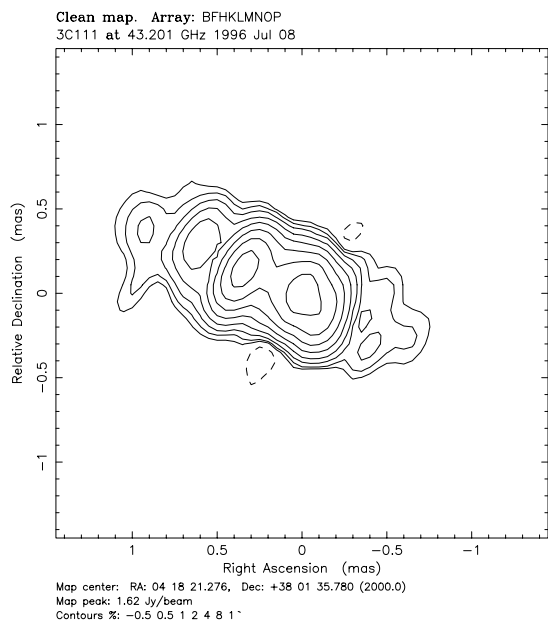
*E. Preuss, W. Alef, K.I. Kellermann (NRAO), and D. Ga uzda (ASC, Moscow)*

3C111 (0415+379) is a classical double-lobed radio source with a well pronounced Fanaroff-Riley type II morphology (Linfield & Perley 1984) associated with an N-type galaxy. The object displays several small-scale features characteristic of a highly active nucleus and is regarded typical for a ‘beamed object’ oriented towards us: it has a prominent superluminally variable parsec-scale radio source with a one-sided jet pointing in the same direction as the one-sided highly collimated ‘VLA-jet’, and a broad line emission region embedded in a starlike nucleus.

3C111 has the strongest compact core at cm/mm wavelengths ( $S \gtrsim 1.5$  Jy) of all FR II radio galaxies, and at times it displays superluminal structural changes and/or strong mm-outbursts. 3C111 is also the nearest of all FR II-type objects with relatively strong compact central components. The spatial resolution achievable with the VLBA + 100m telescope is  $\sim 2.5$  light months at 43 GHz ( $z=0.0485$ ;  $0.65$  pc/mas for  $H_0 = 100$  km/s/Mpc,  $q_0 = 0.5$ ).

Following the large mm-outburst, discovered with the IRAM interferometer in January 1996 (J. Wink, private communication), we observed the object four times within 16 months with the VLBA plus the 100m telescope in the standard polarization mode at 7 mm, the first two times also at 3.6 cm simultaneously. Preliminary total intensity maps at 7 mm (Fig. 14) show an elongated, curved multiple component structure of about 1.1 mas extent, roughly aligned with the large-scale jet. The structure is not of the common ‘core-jet’ type, and there is no unresolved or strongly dominating component in these maps. The significant structural changes between the two epochs cannot be described by a simple kinematic pattern. To obtain a clearer picture of these changes, in the aftermath of the strong mm-outburst, more densely spaced observations are required.

The 3.6 cm brightness distribution (first epoch; not shown here) shows a similar one-sided ‘core-jet’ structure as previous 6 cm maps. The polarized intensity map at 3.6 cm (same epoch) shows the brightest jet component,  $\sim 4$  mas from the core, to be polarized at the 5° level (polarized flux density  $\sim 90$  mJy).



## 2.11 Observations of the nuclei of Giant Radio Galaxies

*R.W. Porcas, D. Graham and A. Patnaik (MPIfR) and Dr. L. Saripalli, (MPIfR and RRI, Bangalore)*

Some of the very largest double-lobed radio sources have projected linear sizes of up to 5 Mpc. VLBI observations of their nuclei may provide clues as to the origins of their large sizes. Initial observations of a sample of “GRG’s” were made with the EVN at 1.6 GHz. The galaxy DA240, with size of 2 Mpc, was shown to have a 2-sided “jet” structure, with a jet/counter-jet flux density ratio of ca. 1, implying either a low Doppler boosting factor, or a very large angle to the line of sight.

More recent observations were made of **DA240**, and the 5 Mpc radio galaxy **3C236**, using the EVN at 5 GHz. These confirm the twin jets in DA240, seen earlier at 1.7 GHz. In 3C236 a single jet is found, pointing to the NW, the side with the shorter core-to-outerlobe distance. However, an “inner lobe” structure reported elsewhere has the asymmetry between core-lobe distances reversed. Investigations of this system are continuing.

## 2.12 Misalignment in core dominated extragalactic radio sources — test of the helical jet model

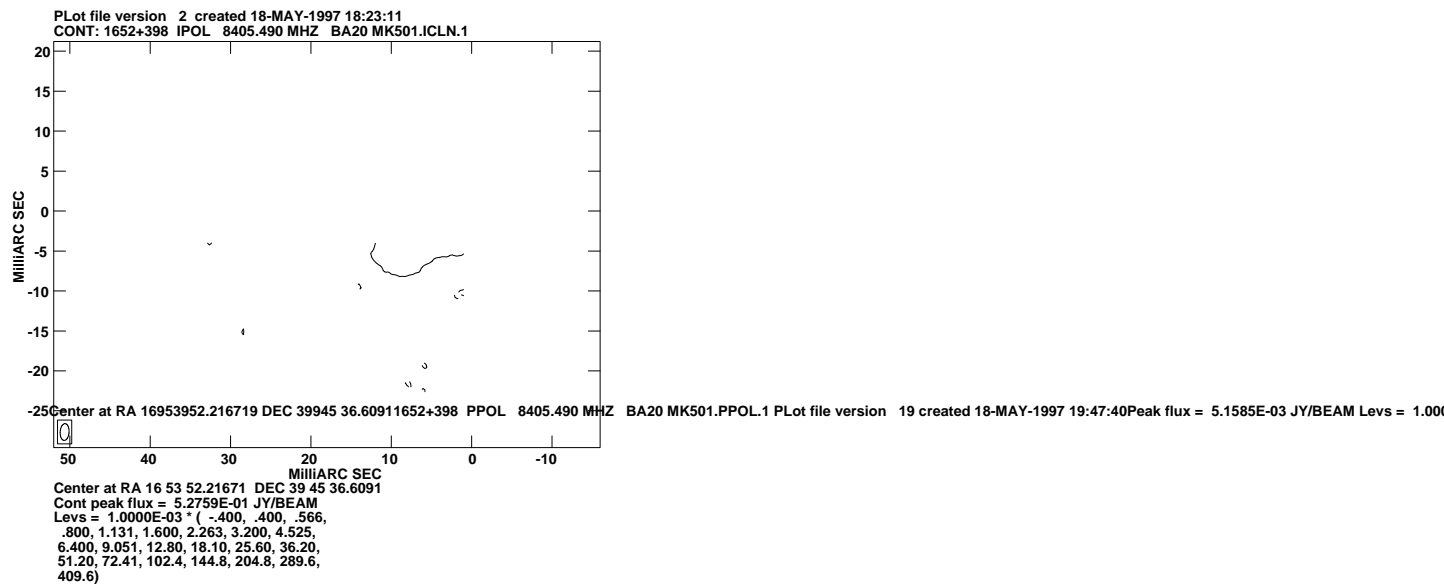
S. Aaron

A well known property of samples of core dominated extragalactic radio sources is the bimodal distribution of the misalignment angle between the VLBI and VLA scale jets, with peaks at  $0^\circ$  and  $90^\circ$ . The misaligned component has been shown to be associated with sources of high optical polarization. The standard model proposed to explain these misaligned jets is the saturated helix model of Conway & Murphy (*Astroph. Journal* **411**:89, 1993). Aaron has been pursuing research to better study these misaligned sources and to test the helical jet model, beginning with observations conducted for his Ph.D dissertation at Brandeis University and continuing during the past year at the MPIfR. For his dissertation, a sample of 16 sources with jet misalignments greater than 60 deg was chosen and studied with the VLBA: 14 in snapshot observations at  $\lambda 18$  cm, and 2 (Mrk 501 and 3C 309.1) at  $\lambda 6$  cm. While the survey was generally inconclusive, some clear results on specific sources were obtained. The images of Mrk 501 demonstrated that the helical jet model fit to a low resolution VLBI image (Conway & Wrobel 1995, *Astroph. Journal* **439**:98) is incorrect; the jet shows several sharp bends in the inner 20 mas, connected by straight jet segments. The polarization properties of these bends suggested they are oblique shocks: intrinsically small bends, possibly arising from deflections by clouds in the ambient gas, amplified in projection. The images of 3C 309.1 revealed a broad region of emission, previously undetected at this frequency. The polarization properties of this emission strongly suggests that it is a lobe-hotspot complex, again implying strong interaction with the ambient gas. Finally, 0814 + 425 was shown to have a very twisted jet, possibly spiral in shape. Several projects have been made in the past year to follow up on this research.

### 2.12.1 Deep VLBA images of Mrk 501

*S. Aaron, J.F.C. Wardle and D.H. Roberts (Brandeis University), A.P. Lo anov (MPIfR)*

New, deep images of Mrk 501 were obtained with the VLBA at  $\lambda 3.6$  cm (see Figure 15). These images show an expanding jet, with a rich polarization structure. The center of the jet is characterized by a parallel electric field, typical for the jets of BL Lacertae objects. However, the edges of the jet are highly polarized with the electric vector orthogonal to the jet direction. This indicates strong shearing of the jet plasma with the ambient gas. Comparison of this image with the earlier  $\lambda 6$  cm image suggests that the outer two bends may have moved, and at superluminal speeds ( $4 - 6 h^{-1}c$ ); the inner two bends have remained stationary. This interpretation is highly speculative because the two images are at different frequencies, and there is therefore the possibility that the core position in the two images is not the same. In collaboration with Andrew Lobanov of the MPIfR, a new project to observe the source simultaneously at many frequencies with a VLBA+VLA+Effelsberg array was proposed and will be observed in the first session of 1998. This project will allow mapping of the rotation measure and spectral turnover frequency distribution across the jet, both being indicators of fluid instabilities and of interactions with the ambient gas.



### 2.12.2 VLBI images of 3C 309.1

*S. Aaron, J.F.C. Wardle and D.H. Roberts (Brandeis University)*

New images of 3C 309.1 were obtained at 1.499, 1.640, 1.662, and 2.263 GHz with a VLBA+VLA array. From these, maps of the rotation measure and depolarization distributions across the source were obtained (Figure 16). These maps confirmed the earlier measurements made from data at  $\lambda$ 3.6 and 6 cm (Aaron, Ph.D thesis) that the rotation measure and depolarization across the source is quite small. Depolarization arises from broad distributions of rotation measure on scales smaller than the synthesized beam, so the lack of depolarization indicates a fairly uniform environment for the source. The source is a prominent example of the Compact Steep Spectrum class of objects. Such sources are believed to be intrinsically small, either due to confinement by a dense medium which depolarizes the radio emission or to a young age. The results of these projects are in conflict with the confinement picture of CSS objects. The strongest evidence of confinement comes from studies of the integrated polarization (*e.g.*, van Breugel, Miley, & Heckman 1984, *Astron. Journal* **89**:5). However, the higher frequency work on 3C 309.1 (Aaron, Wardle, & Roberts 1997, *Vistas in Astronomy*, ed. F. Colomer and M. Garrett, vol. 41, No. 2, 225) has shown that the polarized emission at  $\lambda$ 2 cm and  $\lambda$ 6 cm arises in physically different parts of the source, the high frequency emission from the core and the low frequency from the jet. Hence, a comparison of integrated polarization may not be physically meaningful. Aaron has also mapped the rotation measure across 3C 286 and has collaborated on a similar project on 3C 48. In both sources (CSS objects), like 3C 309.1, the rotation measure is small, with little depolarization.

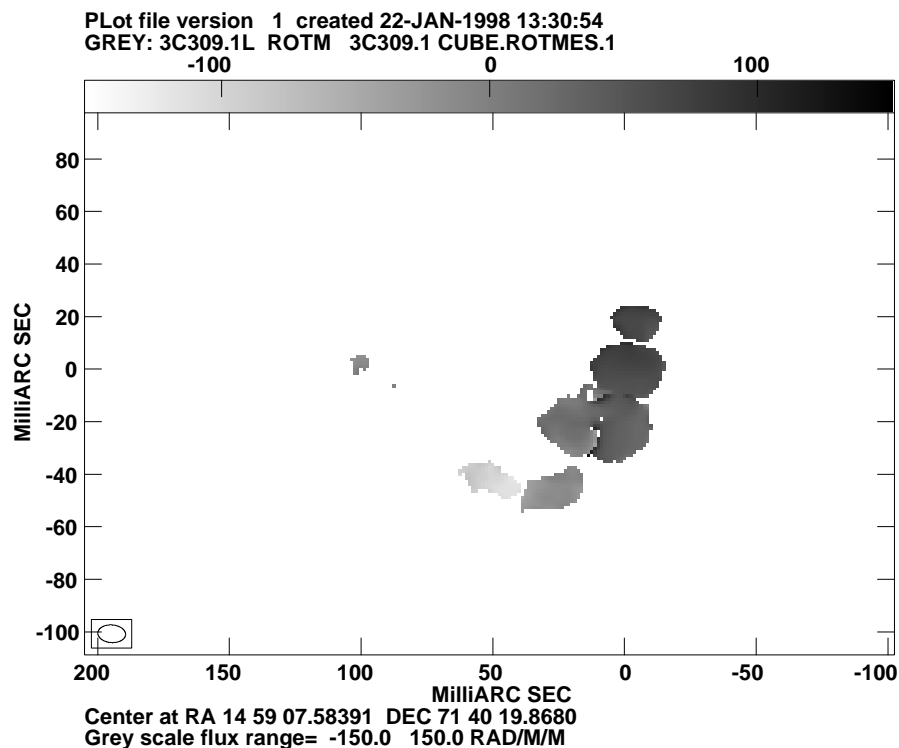


Figure 16: A grey scale plot of the rotation measure distribution in 3C 309.1, made from data at frequencies between 1.499 and 2.263 GHz. The images at all frequencies have been made with a common  $u - v$  range,  $1.88 - 43M\lambda$ , and restored with a common beam size,  $10.55 \times 6.73$  mas oriented at  $86^\circ$ . The grey scale ranges from  $-150$  to  $150$   $\text{rad m}^{-2}$ .



## 2.13 Gigahertz-Peaked-Spectrum (GPS) radio sources

*H. Falcke, A. Marecki, S. Garrington, A. Patnaik*

Using the VLA calibrator survey by Patnaik et al. and other telescopes, Falcke was involved in a search for GPS radio sources which are probably the early stages of radio galaxies and are of potential interest for cosmological questions. 76 new GPS sources were found, thereby substantially enlarging the pool of known GPS sources and providing a useful sample for further studies.

## 2.14 Jets in FR I radio galaxies

*H. Falcke G. & M. Rieke, M. Ward, A.S. Wilson, C. Simpson, C. Henkel, J. Braatz, Y.P. Wang*

In the past Falcke et al. had proposed that the difference between FR I and FR II radio galaxies is in part due to a different kind of molecular torus and they have thought of a number of observational tests for this idea: a search for H<sub>2</sub>O Megamasers in FR I radio galaxies was initiated with a negative result indicating that Megamasers are even harder to detect in FR I radio galaxies than in Seyfert galaxies. Whether this is due to a very turbulent torus (as initially proposed), or a lack of molecular gas, or due to another effect is not quite clear yet. Following another route Falcke et al. searched for broad Pa-alpha emission in FR I radio galaxies in the near-infrared to look for a hidden broad line region, but in this project serendipitously found strong molecular hydrogen emission which seemed to be exclusively associated with radio galaxies with cooling flows. They speculated that this emission might come from molecular gas deposited by the cooling flow and interacting with the radio jets.

## 2.15 Radio Quiet Quasars

*H. Falcke, A. Patnaik, W. Sherwood*

Earlier, Falcke and colleagues had speculated that radio-quiet quasars could have relativistic jets as well. Follow-up observations with Effelsberg, MERLIN, and EVN confirmed several predictions they made, and they found a couple of sources which are most likely relativistically boosted jets in otherwise radio-quiet quasars. If further confirmed, this could have a significant impact on our understanding of AGN, because in this case almost all quasars - rather than only 10% that for example expected source counts of flat- spectrum sources at lower flux levels would change and accretion disk theories would always need to include jet formation.

## 3 Gravitational lenses

### 3.1 Investigating the image morphology of the gravitational lens 2016+112

*R.W. Porcas, M. Garrett (Jodrell, JIVE), S. Nair (Jodrell, RRI Bangalore), and A. Patnaik (MPIfR)*

The gravitational lens effect occurs when the gravitational field of an intervening object (galaxy) distorts the radiation from a distant object. This effect has been recognised in about a dozen radio sources, where multiple images of the background source have been produced. Typical systems result in either 2 or 4 detectable images, each of which is a scaled and distorted image. MG 2016+112 has long been a puzzle; at both radio and optical wavelengths there are at least 2 images, but the nature of a third, elongated radio source in the system has been unclear. Observations were made with the EVN at 5 GHz in 1995, in phase-referencing mode, since the source is weak at this frequency. The two known image components (A and B) were resolved with the 5 mas beam, each showing the double structure of the background object. The third region (C) is revealed to be composed of 4 distinct components, spaced along a gently curving arc. Comparison with previous 1.6 GHz EVN results strongly supports a model in which C consists of 2 further, almost "merging" images of the background double source. Because of the combined effects of a spectral difference between the two components of the background source, and strong differential lens magnification in region C, the spectra of A and B differ significantly from that of C.

### 3.2 Investigation of gravitational lens candidates 1030+074

*R.W. Porcas, A. Patnaik (MPIfR) and E Xanthopoulos, I. Browne, P. Wilkinson (Jodrell Bank)*

A number of surveys have been made at both optical and radio wavelengths to search for new gravitational lens systems, and the Jodrell Bank/VLA astrometric survey has been very successful in producing new candidate systems. 1030+074 is a 1.5 arcsec double source with component flux ratio ca. 15:1. Both are unresolved with MERLIN observations. EVN observations at both 1.7 and 5 GHz were made, with resolutions of 15 and 5 mas respectively. Both components remain unresolved at both frequencies, lending support to the suggestion that both are images of a single, compact background object. Optical observations also confirm that this is a lens system, although the magnification ratio is the highest known to date for a 2-image system.

### 3.3 VLBI Polarimetry of gravitational lens systems

*R.W. Porcas, A. Patnaik (MPIfR) and A. Kem all (NRAO, Socorro)*

VLBI polarimetry provides a powerful tool for investigating the mas structures of gravitational lens images. Both the degree and angle of linear polarisation are unchanged by the lens process itself, and so identification of regions of similar polarisation characteristics in the images can assist in recognising corresponding areas. This in turn can lead to a parametrisation of the action of the lens by an image relative magnification matrix, which provides a constraint for making detailed models of the lens mass distribution. Of course, the observed polarisation properties of the images may be different due to difference Faraday depths along the image paths through the lens galaxy. VLBI polarisation observations have been made of the lens **0218+357**, using the VLBA at 43 GHz, and the VLBA + Effelsberg at 8.4 GHz. Both images in this system show 2 components, in A separated by 1.38 mas in PA 51 deg, in B by 1.47 mas in PA 90 deg. The western, more compact, component in each image appears to be the "core". The 8.4 GHz observations show this to be the most highly polarised component in both images; the observed polarisations angles differ, however, due to the

large difference in Faraday rotation along the 2 image paths. At 43 GHz, the Faraday rotation is negligible, and the polarisation angles are the same, confirming that the lens action itself does not change the polarisation angle, despite the very different structural position angles in the A and B images. Polarisation VLBI observations of other gravitational lens systems have also been made recently, using the VLBA and Effelsberg.

## 4 High precision differential astrometry

### 4.1 Relative astrometry of the quasar pair 1038+52A,B

*R.W. Porcas and M.J.Rioja (MPI, JIVE and Bologna)*

The quasar pair 1038+52A,B are separated by only 33 arcsecs in the plane of the sky, although they have very different redshifts and are thus physically unrelated. Both are strong, compact radio sources. VLBI observations can be made of both sources simultaneously, which allows an analysis to be made of their relative position using VLBI relative phase, since atmospheric and other phase perturbations are common to both sources. Observations made with the VLBA and Effelsberg in 1995 provide a 4th epoch in a series at 2.3/8.4 GHz started in 1981, as well as a first observation at 15 GHz. In addition to providing new maps of both quasars at all 3 frequencies, analysis of the relative position of reference points within the quasars has permitted investigations of the time evolution within the system, and frequency-dependent morphologies. As the two source axes are nearly orthogonal in projection on the sky, it is possible to attribute changes to the quasars individually. Along the quasar B axis direction, the relative position of the A and B “cores” measured at 8.4 GHz has remained constant for 15 years, with an upper-limit to any proper motion of less than about 2 micro-as per year. Quasar A has a prominent, 1-sided jet. Activity within its “core” results in a “jitter” of position along the jet direction, of up to 100 micro-as, but there is no evidence of systematic motion. Quasar A has long been known to exhibit an apparent frequency- dependent “core” position, leading to astrometric separations which differ between 8.4 and 2.3 GHz. The 15 GHz separation is identical to that measured at 8.4 GHz for these epoch 4 observations. A detailed investigation of the effects of the different resolutions at different frequencies lends support to the idea that much of the reported “core shift” with frequency is a resolution effect. The study also shows that even radio components which are apparently optically thin may have spectral sub-structure, and may thus have frequency-dependent positions. A new method of registering the maps at different frequencies for this quasar pair has been suggested.

## 4.2 High precision differential astrometry with closure constraints

*E. Ros, J. M. Marcaide, J. C. Guirado, M. I. Ratner, I. I. Shapiro, T. P. Krichbaum, A. Witzel, R. A. Preston*

Progress has been made in the study of high precision phase-delay differential astrometry through observations of the radio source triangle (Fig. 18) formed by the BL-Lac objects **1803+784** and **2007+777**, and the QSO **1928+738**. The VLBI observations were carried out in November 1991 with an intercontinental array simultaneously at the frequencies of 2.3 and 8.4 GHz. The angular separations of the three radio sources have been determined with submilliarcsecond accuracy from a weighted least squares analysis of the differential phase delay from the three celestial bodies.

This work introduces important advances over previous astrometric studies, carried out for radio source pairs separated by smaller angular distances. The parameters involved in an astrometric VLBI observation have been consistently modeled, in order to reproduce the differential phase observed for radio sources separated by almost  $7^\circ$  on the sky. The possibility of phase-connection over these angular distances at 8.4 GHz has been demonstrated, even at an epoch of a maximum in the solar activity. After the phase-connection, corrections were made for the effects of the extended structure of the radio source and of the ionosphere. This last correction is one of the main technical achievements of the work: it is possible to remove the ionospheric contribution with independent measurements of total electron content of the ionosphere obtained at Global Positioning System (GPS) sites neighbor the VLBI observing stations.

The triangular geometry introduces constraints in parameter space that allow a better estimation of the angular separations among the radio sources. It is possible to test the consistency of the astrometric results through the Sky-Closure, defined as the circular sum of the angular separations of the three radio sources, determined pairwise and independently. In this case it is consistent with zero, and verifies satisfactorily the data process followed.

The comparison of the measurements of the separations of the pair 1928+738/2007+777 (1991 data) with previous measurements (data from 1985 and 1988), carried out with the same technique, allows us to register adequately the absolute position of 1928+738 relative to 2007+777. The proper motion of components in 1928+738 (Fig. 19) is estimated, and also the position of the radio source core is identified. The superluminal motion of the components of 1928+738 is confirmed.

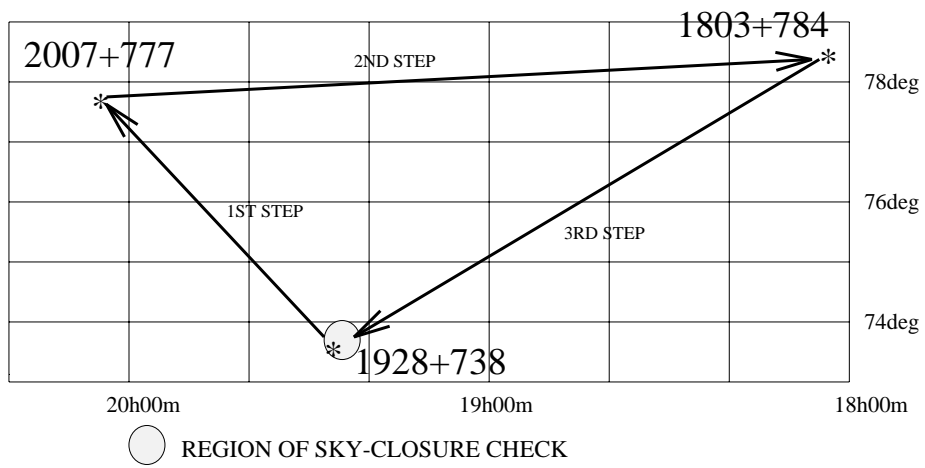


Figure 18: Sky closure test for the triangle 1803+784/2918+738/2007+777.

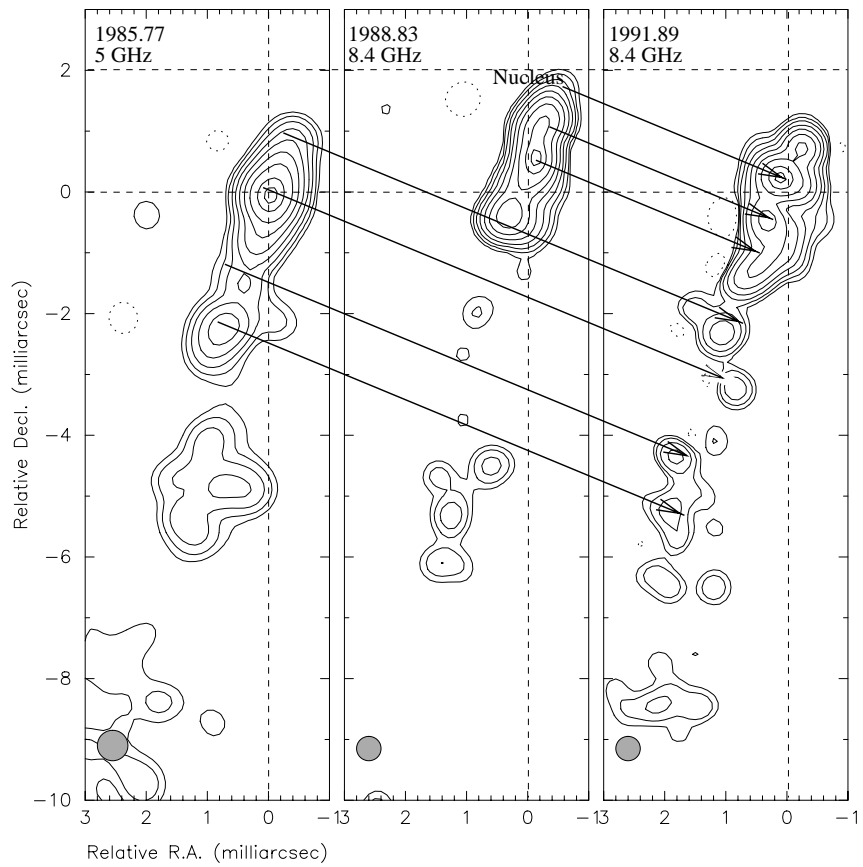


Figure 19: Proper motions in 1928+738. The alignment of the maps is done with the astrometric results.

## 5 Nearby galaxies

### 5.1 Compact radio cores in nearby galaxies

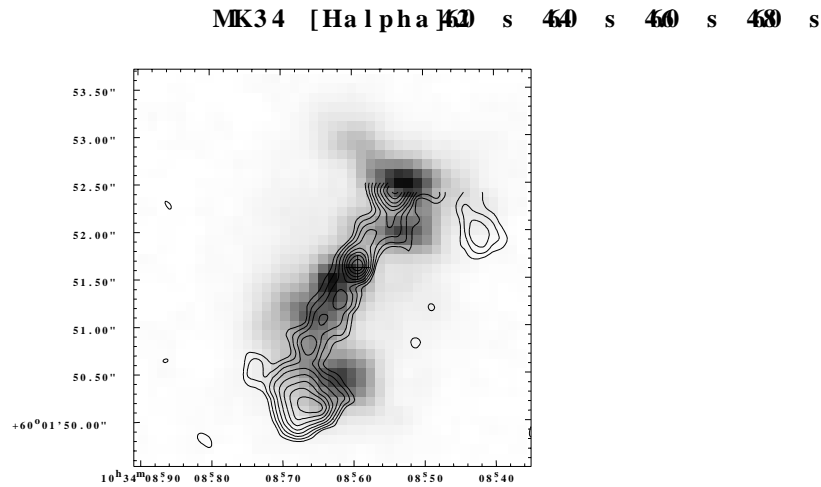
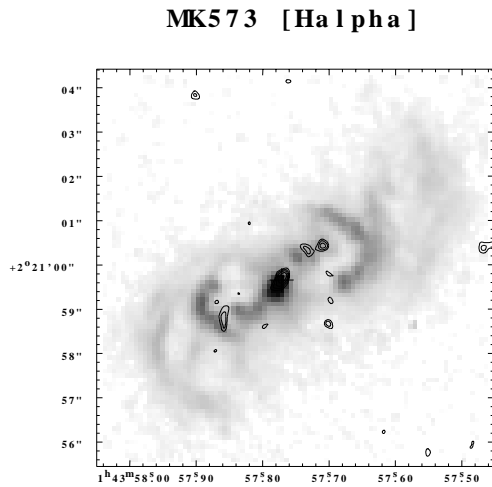
*H. Falcke, L.C. Ho, A.S. Wilson, J. Ulvestad*

Over the last years Falcke has developed a model for compact radio cores in nearby galaxies which explains them as scaled down versions of jets in AGN. The alternative model currently under discussion for these radio cores is the advection dominated accretion flow (ADAF) solution (inflow) even though in most cases it does NOT fit the observed radio data well and there is clear evidence for jets at least in some cases. Falcke has used the **VLA to survey a sample of nearby low-luminosity AGN (LINER galaxies) at 2cm** and found compact, flat spectrum cores in at least a quarter of the galaxies surveyed. In contrast to the extended radio emission, the radio core flux scales well with the emission-line flux from the AGN. The brightest of these radio cores are currently being studied with the VLBA to look for indications of jet structures and an additional, larger sample will be surveyed by the VLA soon.

## 5.2 Seyfert galaxies of type 2

*H. Falcke, A.S. Wilson, C. Simpson*

Falcke has worked on a sample of Seyfert 2 galaxies observed with the HST (Fig. 20); the galaxies were also observed by the VLA where they found the clearest evidence yet for the strong influence the jets in Seyferts have on the narrow-line region: morphology and kinematics of the hot gas in Seyferts cannot be understood without taking the radio jets into account! A number of follow-up programs are under way which try to further investigate the properties of jets in Seyfert galaxies, including MERLIN, VLA, and VLBA observations.



## 6 The Galactic Center

### 6.1 Spectrum of Sgr A\*

*H. Falcke, W.M. Goss, H. Matsuo, P. Teuben, J.-H. Zhao, R. Zylka*

A campaign to measure the simultaneous radio spectrum from 20cm to 1mm of the supermassive black hole candidate Sgr A\* at the Galactic Center was organized and led by H. Falcke. The campaign involved four different telescopes on three continents and demonstrated that there is a mm-bump in the spectrum, requiring a compact synchrotron component in this source with a size of only a few gravitational radii of the black hole. Using the most recent and very precise measurements of the mass of Sgr A\*, they argue that future VLBI observations at 1mm will not only be able to resolve this source, but will even enable us to see the photon horizon of this black hole and therefore finally prove (or disprove) the predictions of General Relativity in the strong limit.

### 6.2 Sagittarius A\*

*G. Bower, Backer, Wright (UCB), Doeleman, Rogers (MIT)*

The compact, non-thermal radio object in the Galactic Center, Sgr A\*, is the nearest example of an active galactic nucleus. However, it is obscured by a thermal plasma. Observations at high frequencies — where the effect of scattering is the least — provide the best opportunity to study the central object. Bower and Backer observed Sgr A\* with the VLBA at the shortest wavelength available on that array, 7 mm. This represents the highest-frequency completely-sampled image available of Sgr A\*. The image is dominated by the scattering properties. The intrinsic source of radiation must be smaller than 4.1 AU. Combined with dynamical measurements in the infrared and the radio, this provides a very convincing argument that Sgr A\* is a black hole with the mass of one million (or more) Suns. These results are accepted for publication in ApJL in 1998.

Bower, Backer, Wright, Doeleman and Rogers also observed Sgr A\* at a wavelength of 3 mm with an array of 4 US millimeter observatories, Haystack Observatory (MA), Kitt Peak Observatory (AZ), Owens Valley Observatory (CA) and Hat Creek Observatory (CA). The results are consistent with those at lower frequencies, indicating that the intrinsic size of Sgr A\* must be smaller than 1 AU.

## 7 Stars

### 7.1 VLBI measurement of the size of dMe stars

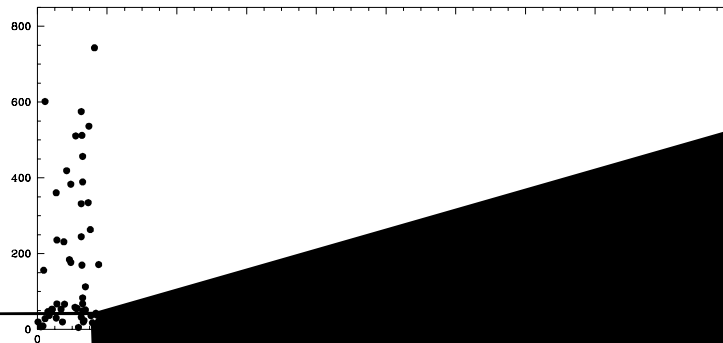
*W. Alef, A.O. Benz (ETH Zürich), and M. Güdel, (Paul-Scherrer-Institute, Villingen, CH)*

The binary system YY Gem, which consists of two dM1e stars, has been observed using intercontinental Very Long Baseline Interferometry (VLBI) at 1.6 GHz during an eclipse. The stellar emission was at a low, quiescent level at all observing periods. The correlated flux decreases slightly with baseline length, indicating that the source is resolved at the longest baselines. This is confirmed by model fits, which give a FWHM size of 1.05 mas ( $2.2(\pm 0.5) \cdot 10^{11}$  cm or  $2.4 \pm 0.6$  photospheric diameters) for the radio emitting source. A lower limit to the size derived from the lack of observable eclipse effects agrees with this value. The resulting brightness temperature of  $9.0 \cdot 10^8$  K is compatible with gyrosynchrotron emission. Deviations from circular symmetry are only marginal. The loops that trap the radio emitting electrons reach an altitude of at least  $3.7 \cdot 10^{10}$  cm, suggesting that the surface is covered with many, large active regions.

## 7.2 Activity cycles in UX Arietis — comparison with the Sun

*M. Massi, J. Neidhöfer, G. Torricelli-Ciamponi, F. Chiuderi-Drago*

By analysing long term radio observations (performed with the Effelsberg 100-m telescope) of the binary system UX Arietis activity cycles have been discovered, which are strongly reminiscent of those present in the Sun. It is well known that the activity cycle in the Sun is 11 years, while the general magnetic field reverses every 11 years, returning to its initial configuration after 22 years, namely after two consecutive cycles of activity. Now it has been discovered in UX Arietis an activity cycle of 25.5 days during which the polarization reverses and returns to its initial value after about two consecutive cycles of activity. Moreover as the cycle of 11 years of the Sun is modulated with a period of 90–110 years, poorly estimated due to its long term occurrence, it has been found that the 25.5 days activity cycle in UX Arietis is also modulated with a period of 158 days. In Fig. 21 are shown the radio light curves produced by folding the data with the specified periods. The solar activity cycle is related to the dynamo at work in the sun's interior. The fact of having in UX Arietis the same phenomena as in the Sun but at much shorter time scales (i.e. days instead of years) should make possible to acquire better statistics in the future and improve our understanding of the dynamo processes. Figure 21: Ra



### 7.3 VLA observations of the field around the X-ray binary LSI+61303

*M. Massi*

Deep VLA observations at 6 cm of the field around the radio emitting X-ray binary LSI+61303 have been carried out in an attempt to search for associated extended radio emission. The result is that the many detected clumps are very likely free-free radio emitting material from the nearby giant HII region W4 (see Fig. 22).

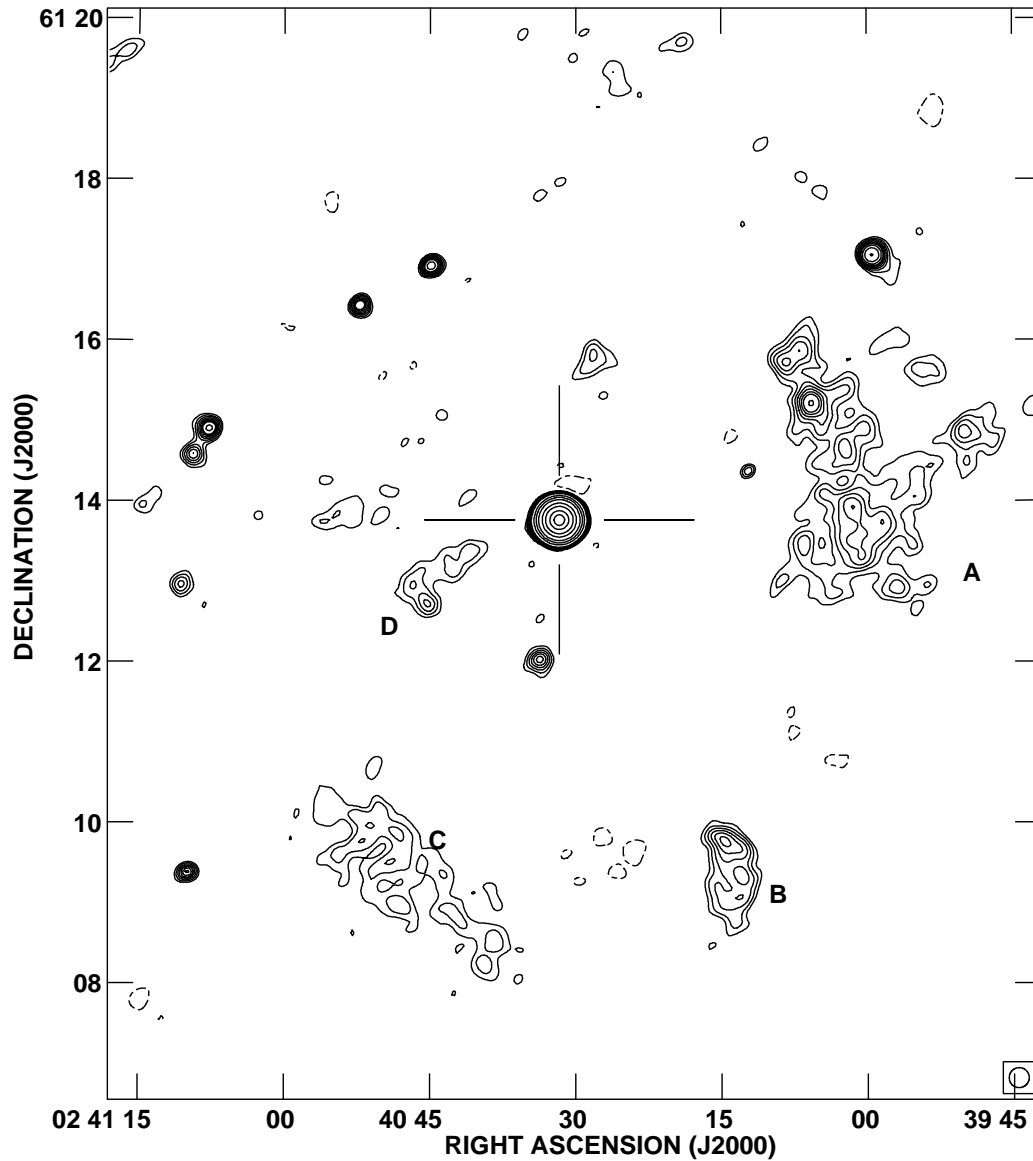


Figure 22: VLA map of the X-ray binary LSI+61303 at 6 cm. The synthesized beam is 15" x 15".

## 8 VLBI techniques

### 8.1 Total Power Corrections for Atmospheric Phase

*G. Bower, Backer, Wright, Plambeck (UCB), Graham, Krichbaum (MPIfR) and Conway (Onsala)*

Water vapor in the atmosphere causes variations in the measured interferometer phase on time scales of seconds. This leads to decorrelation and a significant loss of sensitivity. Bower, Backer, Wright and Plambeck have investigated the application of this technique at 3 mm with the Hat Creek and Kitt Peak telescopes and found it viable given sufficient receiver sensitivity. This work was published in *Journal of Geophysical Research*.

Bower, Graham, Krichbaum and Conway are currently investigating the application of this technique to the Effelsberg, Pico Veleta and Onsala telescopes.

## 8.2 Discovery of a systematic error in EVN VLBI

*M. Massi, S. Aaron, D. Gabuzda, K. Leppanen, L. Moscadelli, M. Rioja, K. Ruf, H. Sanghera*

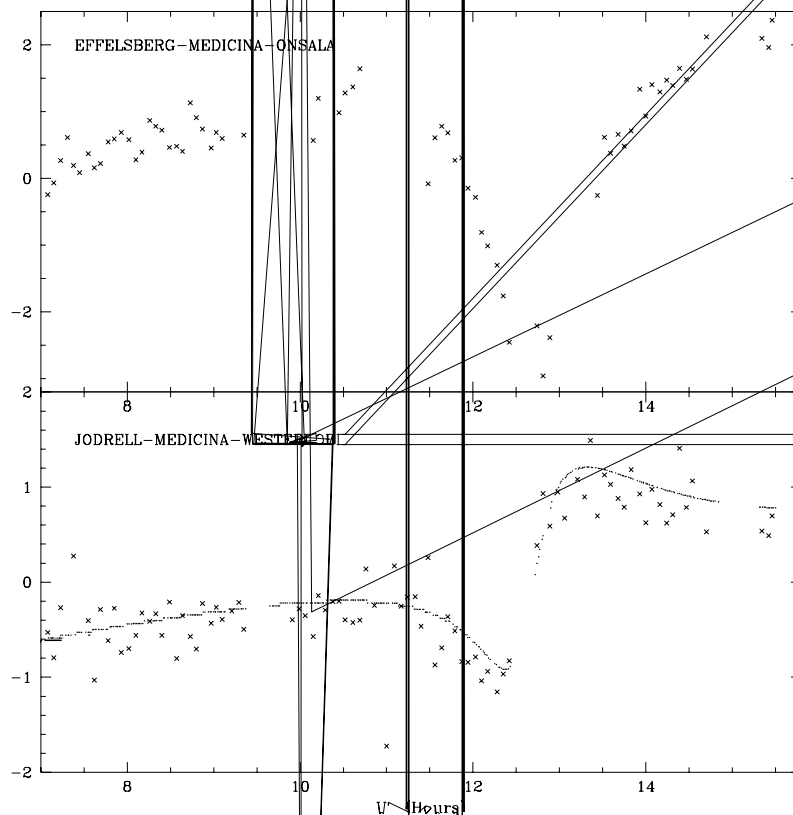
A systematic error in VLBI measurements made with European telescopes has been discovered. The origin of the error lies in the high instrumental polarization of some of the network antennas. This has been proved by the excellent agreement found between the error function (i.e. the closure phase of a point-like source) and a model based on the effects of the instrumental polarization. These effects have been thought up to now to be completely negligible because they affect the measurements only in the second order. On the contrary the high instrumental polarization at some telescopes makes this error much higher than the noise.

The result of this work is an improvement by a factor 7 in dynamic range of the images obtained from European VLBI data.

Leppanen, K., Massi, M., Rioja, M., Sanghera, H., 1997, *Vistas in Astronomy*, vol. 41, Part 2

Massi, M., Rioja, M., Gabuzda, D., Leppanen, K., Sanghera, H., Ruf, K., Moscadelli, L. 1997, *AA Letters* 1, 318, L32

Massi, M. and Aaron, S. 1997, EVN Document 75



### 8.3 Calibration of the instrumental polarization of VLB interferometers

*M. Massi, M. Aaron, G. Tuccari, S. Orfei*

The calibration of the instrumental polarization of an interferometer requires the estimation of parameters called 'D' terms. Such an estimation requires quite complex and time consuming VLBI observations. In order to simplify this procedure, two different investigations have been started. The first is to try to monitor the D terms at each telescope equipped with a polarimeter by performing single-dish observations (i.e. without the necessity of VLBI observations). The exact mathematical relationship between single-dish instrumental polarization and interferometric instrumental polarization (i.e. the D terms) has been determined.

The second investigation is to try to establish the degree of variability of the D terms with time. Therefore a set of four observations at  $\lambda = 6$  cm has been performed in 1997. An important finding